Int. J. Electrochem. Sci., 2 (**2007**) 958 - 972

International Journal of ELECTROCHEMICAL SCIENCE
www.electrochemsci.org

Solute-Solvent Interactions from Admittance Measurements: Potential Induced and Water Structure-Enforced Ion-Pair Formation

C. V. Krishnan[1,2,*], *M. Garnett*[1] *and B. Chu*[2]

[1] Garnett McKeen Lab, Inc., 7 Shirley Street, Bohemia, NY 11716-1735, USA
[2] Department of Chemistry, Stony Brook University, Stony Brook, NY11794-3400, USA
[*]E-mail: ckrishnan@notes.cc.sunysb.edu

Received: 29 August 2007 / *Accepted:* 5 September 2007 / *Online published:* 20 October 2007

Admittance measurements of aqueous 0.010, 0.10 and 1.0 M sodium chloride solutions and 0.010 M solutions of other sodium halides were investigated using a mercury working electrode. The measurements indicated a decrease or increase in admittance with decreasing frequency, depending on the concentration of sodium chloride and the range of the scanning potential. As the potential changes from negative to less negative, to zero and finally to positive, the admittance increased and passed through a maximum. There was also a slight anodic shift in the maximum with decreasing frequencies, suggesting the role of solute-water interactions and orientation effects of water near the double layer changeover potential. To explain the admittance data of NaF, NaCl, NaBr, and NaI, we have proposed a new model, "potential induced and water structure-enforced ion-pair formation", at or near the double layer. A comparison of the concentration dependence of the admittance data for NaCl suggested that this type of ion-pair formation was also favored even in very dilute solutions at or near the double layer, contrary to the normal electrolyte behavior in bulk. The present model also points out the need to modify the current models employed to explain the differential capacitance and the surface excess entropy data.

Keywords: admittance, potential-induced and water structure-enforced ion-pair, Gurney co-sphere

1. INTRODUCTION

Our interest in aqueous sodium chloride was necessitated by recent interests in biological electronic circuits involving DNA (or RNA or proteins)-salt-water interactions. We have chosen mercury as the working electrode because past electro-capillary measurements for different electrolytes were primarily being carried out using mercury. Also, it was relatively easy to get a fresh drop of mercury each time and thus to minimize surface inhomogeneities. The mercury drop approach also offered opportunities to study the influence of surface area more easily because the size of the

drop could be easily changed. We had reported earlier results of proteins, collagen and prothrombin, and observed the profound influence of NaCl on their electronic behavior [1, 2]. While NaCl promoted the electronic behavior of collagen, it was detrimental on prothrombin as evidenced by the occurrence of impedance loci in the first two quadrants, a characteristic of negative differential resistance and probable resonant tunnel diode behavior. We had also reported the admittance and impedance behavior of aqueous 0.010 M KCl, KBr, and KI using a static mercury drop electrode [3]. As expected, the interaction of mercury was observed to increase from chloride to bromide to iodide near the passivation region. Both p-type and n-type semiconduction in these systems could be observed from Mott-Schottky plots.

Differential capacity measurements and electrocapillary measurements of alkali halides, their mixtures, and tetraalkylammonium iodides have been utilized to study the nature of specific adsorption at the double layer [4-7]. It has been found that for small monatomic ions, the differential capacity of the inner part of the double layer is not sensitive to the nature of the cation except in the region of high cathodic polarization. Our recent impedance measurements of potassium halides have revealed the structural effects of water and solute-solvent interactions near the double layer [3]. Also our impedance measurements of biological molecules such as collagen [1] and prothrombin [2] along with our more recent admittance measurements of molybdates at different pH values [8] and peroxomolybdate solutions [9] have indicated the promising potential of admittance measurements for obtaining information on solute-solvent interactions at or near the double layer.

Admittance (Y) is the inverse of impedance (Z) with $Y \equiv Z^{-1} \equiv Y' + jY''$. From its introduction in 1969 by Bauerle for the determination of conductivity of solid electrolytes [10], no serious attempts have been made to utilize this concept. Apart from a few passing comments on admittance in textbooks as well as reviews on impedance spectroscopy, we are not aware of any literature highlighting its importance. Our past measurements have pointed out its many potential uses. In this report we present its application to one of the simplest electrolytes, sodium halides.

2. EXPERIMENTAL PART

An EG & G PARC Model 303A SMDE tri-electrode system (mercury working electrode, platinum counter electrode and Ag/AgCl (3.5M KCl, reference electrode) along with Autolab eco chemie was used for cyclic voltammetric and electrochemical admittance measurements at 298 K. Sigma NaCl and distilled water were used for preparation of all solutions. The solutions were purged with N_2 for about 10 minutes before the experiment. Admittance measurements were carried out using about 7 mL solutions in the frequency range 10,000 Hz to 25 mHz. The amplitude of the sinusoidal perturbation signal was 10 mV.

3. RESULTS AND DISCUSSION

3.1. Cyclic Voltammetry

These measurements were made for 0.010 M, 0.10 M and 1.0 M aqueous NaCl solutions at a scan rate of 100 mV/s in the potential range 0.3 to -1.0 V. There was no noticeable activity in the scan

range 0 to -1.0 V. The results shown in Figure 1 indicated the interaction of the chloride and consequent passivation of mercury.

There was an increase in both cathodic and anodic currents with increasing concentration of the chloride. Also both the cathodic (0.097, 0.083, and 0.034 V) and anodic (0.202, 0.146, and 0.092 V) peaks were shifted to more cathodic potentials with increasing concentration of the chloride indicating an increase in interaction.

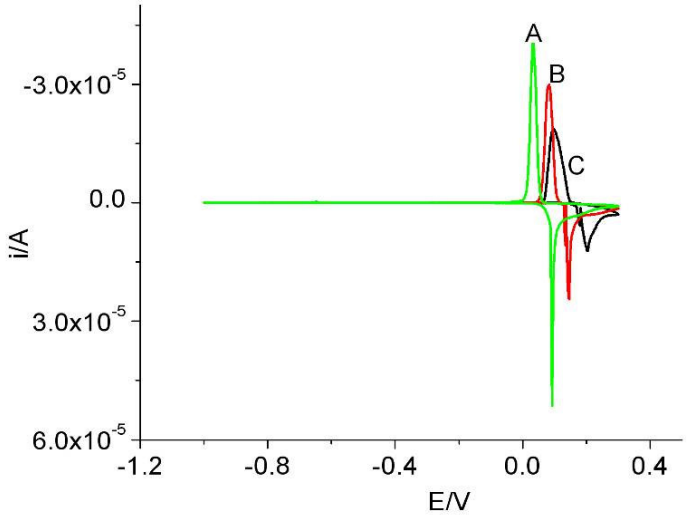

Figure 1. Cyclic voltammetry curves of 1.0 M (A), 0.10 M (B) and 0.010 M (C) solutions of aqueous sodium chloride. Scan from 0.3 to -1.0 V and back. Results of the third scan are shown in the figure.

3.2. Admittance

The admittance data for 1.0 M aqueous NaCl shown in Figure 2 indicated several interesting features: 1. In the extreme cathodic range, the admittance decreased continuously with decreasing frequency. 2. In the intermediate cathodic range, the admittance increased with decreasing frequency up to 3000 Hz and then decreased with further decrease in frequency. 3. In the cathodic potential range close to zero, the admittance shoulder increased with decreasing frequency and then stayed nearly the same for the frequencies 2000 and 1000 Hz. 4. The first admittance maximum near -0.73 V for 10,000 Hz shifted to the anodic side by about 100 mV each for 5000 and 3000 Hz while the maximum was growing. With further decrease in frequency, the admittance decreased without further anodic shift in the maximum. 5. When the first admittance maximum was shifting to more anodic potentials, a second maximum or shoulder was growing near potential zero. When there was no anodic potential shift in the first admittance maximum, the second one shifted to the anodic side by about 60 mV with further decrease in frequency. 6. The sharp change in admittance at about 0.08 V became less and less with decrease in frequency and was not noticeable at 1000 Hz. Probable explanations for these and following observations are included at the end of this section and in section 3.3.

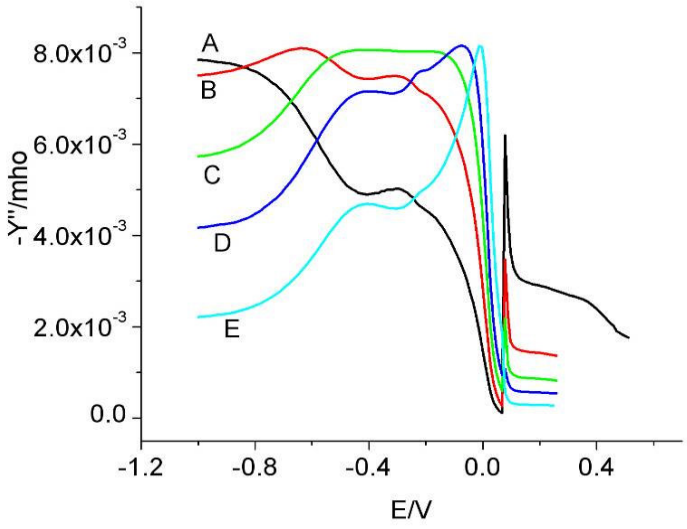

Figure 2. Admittance of 1.0 M aqueous NaCl; A, 10000 Hz; B, 5000 Hz; C, 3000 Hz; D, 2000 Hz; E, 1000 Hz

The admittance data for 0.10 M NaCl in the frequency range 10000 Hz to 1000 Hz are shown in Figure 3. Contrary to the behavior of 1.0 M NaCl, the admittance increased with decreasing frequency except for 1000 Hz in the high cathodic range. The first admittance maximum or shoulder seen for 1.0 M NaCl became less sharp for 0.10 M solutions. Also it was appearing at more anodic potentials and at the same time shifting to more anodic potentials with decreasing frequencies. Another interesting feature was that the second admittance shoulder near 0.0 V did not level off. While the sharp change in admittance at 0.08 V was not noticeable for 1.0 M solutions at 1000 Hz, it was noticeable for all the frequencies for 0.10 M solutions at 0.128 V.

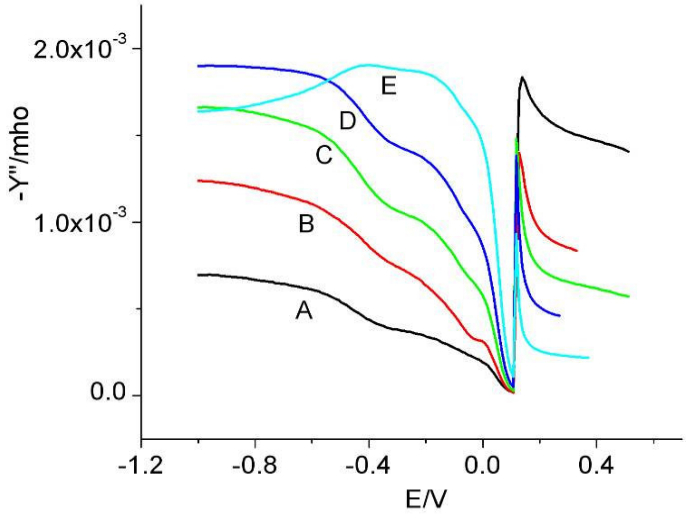

Figure 3. Admittance of 0.10 M aqueous NaCl; A, 10000 Hz; B, 5000 Hz; C, 3000 Hz; D, 2000 Hz; E, 1000 Hz

The admittance data for 0.010 M NaCl in the frequency range 10000 Hz to 1000 Hz are shown in Figure 4. The admittance increased uniformly with decreasing frequencies throughout the range of 10000 to 1000 Hz and was mostly similar to the behavior in 0.10 M solutions. The first admittance shoulder or maximum was at more anodic potentials than observed in 1.0 M or 0.10 M solutions. Similar to the behavior in 0.10 M solutions, the sharp change in admittance at 0.168 V was noticeable for all the frequencies from 10000 to 1000 Hz. At this concentration, there was more scatter in the data at the highest frequencies.

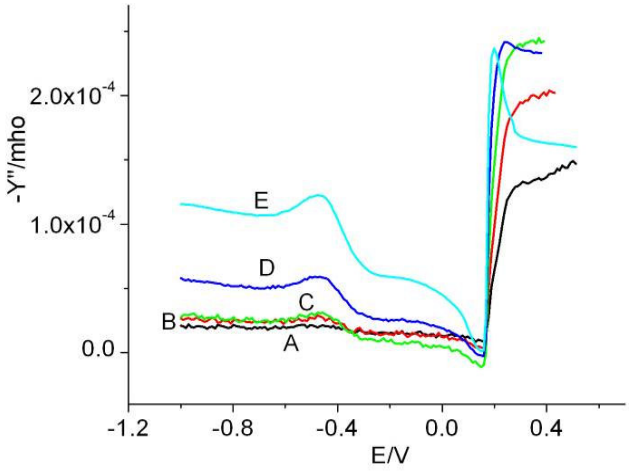

Figure 4. Admittance of 0.010 M aqueous NaCl; A, 10000 Hz; B, 5000 Hz; C, 3000 Hz; D, 2000 Hz; E, 1000 Hz.

The admittance data for 1.0 M aqueous NaCl in the frequency range 1000 Hz to 50 Hz are shown in Figure 5. For the sake of continuity, the 1000 Hz data are included Figure 5. It was observed that the admittance decreased uniformly with decreasing frequency and the maximum near 0.0 V stayed nearly the same initially while shifting to anodic potentials by a few milli volts. When the frequency decreased below 250 Hz, there was a decrease in the admittance maximum value, and there

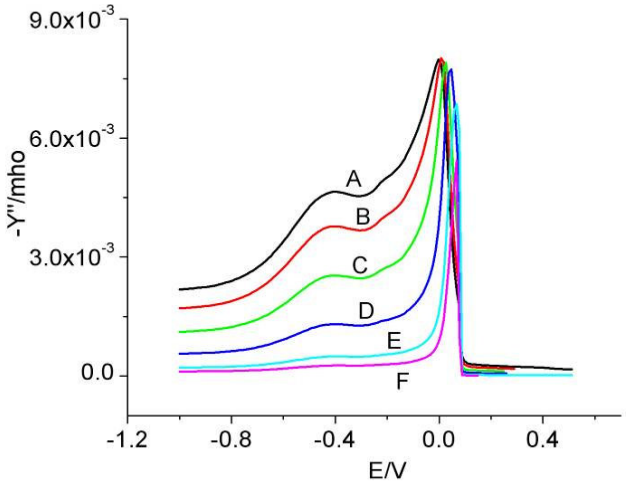

Figure 5. Admittance of 1.0 M aqueous NaCl; A, 1000 Hz; B, 750 Hz; C, 500 Hz; D, 250 Hz; E, 100 Hz; F, 50 Hz

was still a continuing small anodic potential shift in the maximum. The dramatic sharp shift in admittance observed at 2000 Hz and above at 0.08 V was not observed here.

The admittance data for 0.10 M aqueous NaCl shown in Figure 6, are mostly similar to the behavior for 1.0 M solution in that there was a continuous decrease in admittance with decreasing frequency in the high cathodic voltages and a slight shift in the admittance maximum near 0.1 V to the anodic potential side. Near the potential of the second admittance maximum, the admittance increased throughout with decreasing frequency. While a sharp change in admittance was observed in 1.0 M solutions at 0.08 V up to 2000 Hz, a similar sharp change was observed here at 0.128 V for frequencies 1000, 750 and 500 Hz.

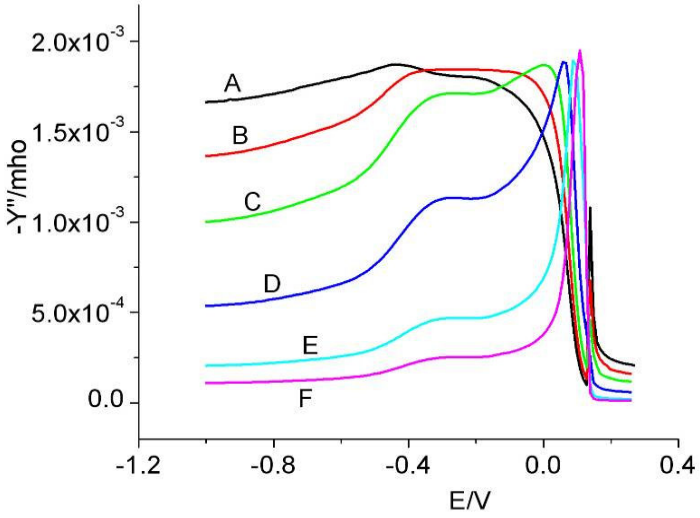

Figure 6. Admittance of 0.10 M aqueous NaCl; A, 1000 Hz; B, 750 Hz; C, 500 Hz; D, 250 Hz; E, 100 Hz; F, 50 Hz

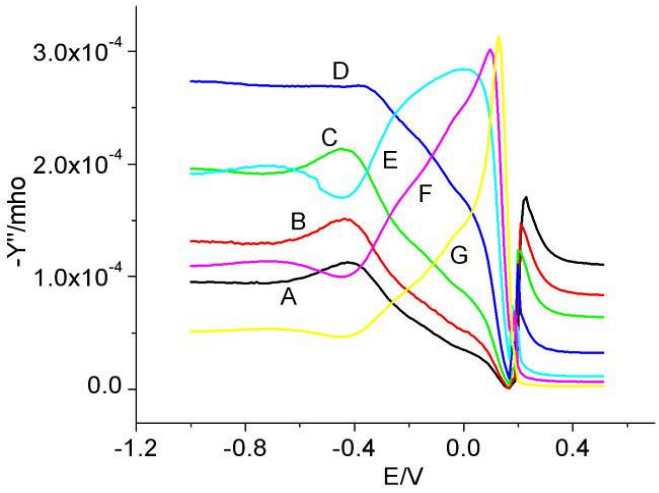

Figure 7. Admittance of 0.010 M aqueous NaCl; A, 1000 Hz; B, 750 Hz; C, 500 Hz; D, 250 Hz; E, 100 Hz; F, 50 Hz; G, 25 Hz

The admittance data for 0.010 M aqueous NaCl in the frequency range 1000 Hz to 25 Hz are shown in Figure 7. The admittance increased with decreasing frequency from 1000 Hz to 250 Hz throughout the cathodic potential range. With a further decrease in frequency, the admittance decreased in the most cathodic potentials. However, at potentials close to zero and beyond, the admittance increased. Also the anodic shift observed for the admittance maximum in Figures 5 and 6 are also observed here. While a sharp change in admittance was observed in 1.0 M solutions at 0.08 V up to 2000 Hz, and for 0.10 M solutions at 0.128 V for frequencies 1000, 750 and 500 Hz, a similar sharp change in admittance was observed here for frequencies from 1000 to 25 Hz.

For the purpose of comparison, the admittance data at 1000 Hz for NaCl at differing concentrations are shown in Figure 8 (left side). To highlight the effects, the data for 0.010 M and 0.0010 M are replotted in Figure 8 (right side). The data clearly demonstrate a decrease in admittance as the potential approaches zero volt and these decreases were shifted to more cathodic potentials with decreasing NaCl concentration.

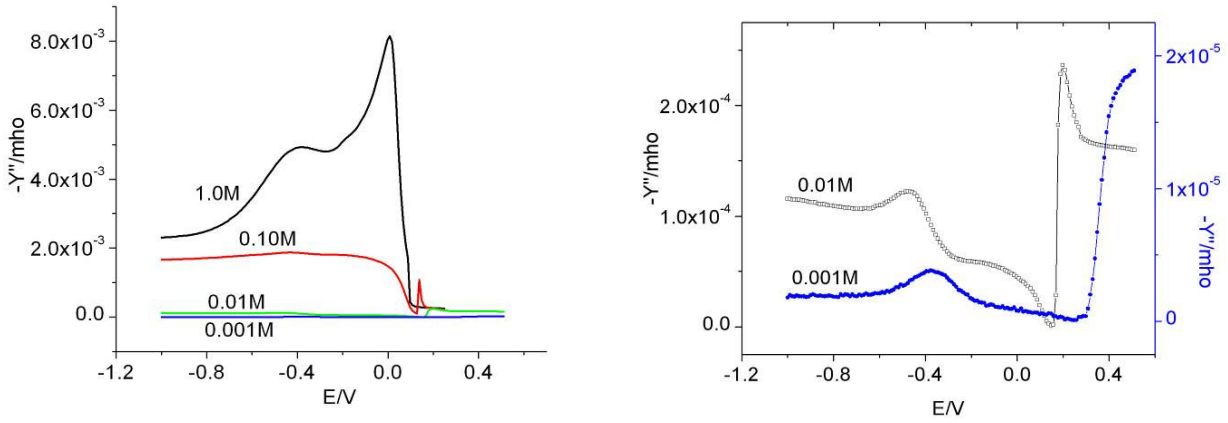

Figure 8. Admittance comparison: 1000 Hz, sodium chloride at different concentrations

To compare the effect of halide on the observed behavior, the admittance data for 0.010 M solutions of sodium halides at 1000 Hz are shown in Figure 9. These data demonstrate that the decrease in admittance at potentials close to zero shifts to more cathodic potentials as the size of the anion increases, viz., the decrease is in the order NaI > NaBr > NaCl > NaF. We have focused on the admittance results at cathodic potentials. The last anodic peak (at 0.08, 0.128 and 0.168 V for 1.0, 0.1 and 0.01 M solutions) followed by a leveling off in admittance was observed for every concentration and is attributed to the passivation of mercury. This peak is shifted to more anodic potentials with a decrease in the concentration of NaCl. These observations are consistent with the observed peaks in the cyclic voltammograms. We plan to discuss this part of admittance curve and the corresponding impedance data in a later report. We do not have differential capacitance data or surface excess entropy data available from the literature at different frequencies. We also do not have admittance data for simple electrolytes except our own reported data for potassium halides. The observed admittance behavior can be broadly classified into three potential regions, -1 to -0.8 V, -0.8 to -0.3 V and -0.3 to about 0.0 V, and two frequency regions, 10,000 to 1000 Hz and below 1000 Hz.

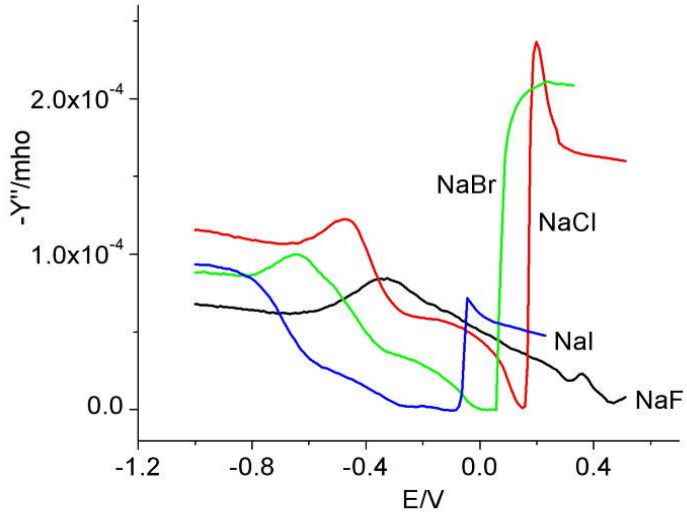

Figure 9. Admittance comparison: 1000 Hz, 0.010 M sodium halides.

In the potential range -1 to -0.8 V, the admittance decreases with decreasing frequency for 1.0 M solution whereas the admittance increases with decreasing frequency for 0.10 and 0.010 M solutions. Since we know that the double layer concentration of the electrolyte is about 10 times higher than that in the bulk, we have to assume that the hydration co-sphere overlap effects and the consequent changes in orientation of water with changing frequencies are more dominant at lower concentrations of NaCl as expected (see section 3.3).

In the potential range of -0.8 to -0.3 V, the behavior is somewhat similar for all solution concentrations, in that the admittance increases with decreasing frequency.

In the potential range of -0.3 to about 0.0 V, the admittance for 1.0 M solution increases and reaches a maximum around 3000 Hz, whereas the admittance maximum for 0.10 M solution is around 750Hz and that for 0.010 M solution it is at about 100 Hz. To explain this observed increase in admittance at decreasing frequencies we suggest two possibilities. 1) there must be considerable hydrogen bond breaking in the diffuse layer and consequent increase in mobility for ions. This is possible because around this potential range the orientation of the ions towards mercury has to change from sodium to chloride. This forces corresponding changes in the orientation of the water molecules in the hydration layer. 2) The second possibility is dissociation of the ion-pairs formed (see discussion in the next section). If there is considerable hydrogen bond breaking, there is no need for the potential induced and water structure-enforced ion pair formation in this potential region.

3.3. Double Layer Structure and Ion Pair Formation

In order to understand the double layer behavior, it is essential to have a bird's eye view of the bulk electrolyte solution behavior. To explain the conductance behavior as well as the osmotic and activity coefficient data of electrolytes, at least three kinds of ion pair formation have been proposed in the literature [11-15]. A simplistic view of those three kinds of ion-pairs is shown in Figure 10. The

Coulombic type ion-pair or Bjerrum type ion pairs are assumed to be formed when their energies of mutual electrical interaction are considerably higher than their thermal energy. According to Bjerrum, " the average effects of ion pair formation may be calculated on the basis that all oppositely charged ions within a certain distance of one another are associated into ion pairs, though in reality a momentarily fast-moving ion might come within this distance of another and pass by without forming a pair" [11]. This critical distance, q, is given by the equation:

$$q = | z_1 z_2 | e^2/[2\varepsilon kT]$$

where z_1 and z_2 are the charges on the ions, e is the protonic charge, ε is the dielectric constant, k is the Boltzmann constant and T is the absolute temperature. For a 1:1 electrolyte in water at 25 ^{o}C, q = 0.357 nm. On the other hand Fuoss assumed ion-pair formation only if the ions were in contact with no intervening solvent [12]. Whatever the definition of this type of ion-pair should be, it is consistent with the observed trend in activity coefficient data at a given concentration, viz., Li > Na > K > Rb > Cs for the halides and these are in the order of decreasing hydration of the cations from Li to Cs.

Ion-pair formation through a polarized water molecule, called localized hydrolysis, was introduced [13] to explain the reversal in the order of osmotic and activity coefficient data of hydroxides and acetates of ions such as lithium. In this case, the observed order was Cs > Rb > K > Na > Li. By this hypothesis the strongly hydrated lithium ion interacts with a proton acceptor, such as hydroxide or acetate, through a highly polarized water molecule. This kind of ion pairing has also been used to explain the order of activity coefficients of the smaller alkali halides, such as LiI > LiBr > LiCl [14].

The positive deviations of osmotic and activity coefficient data of 1:1 electrolytes from the Debye-Huckel limiting laws at higher concentrations has been attributed to ion hydration effects.

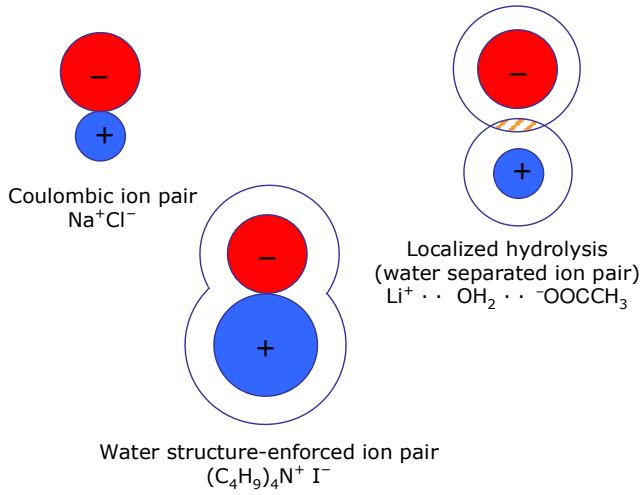

Figure 10. Ion-pair formation in aqueous solutions

The water structure-enforced ion-pair formation was introduced to explain the osmotic and activity coefficient data of large ions such as tetraalkylammonium iodides [15]. When both cation and anion are large, unhydrated, and univalent, the hydrogen bonded water structure forces the formation of ion-pairs in order to maximize water-water hydrogen bond interactions and minimize structure breaking. This is different from the traditional Coulombic ion-pairing where oppositely charged small ions form the ion-pair. This kind of ion-pairing has also been used to explain the behavior of large cations on differently cross-linked strong acid ion exchangers as well as the anion exchange behavior of large anions [16-17].

A pictorial and simplified view of how these three different kinds of ion-pairs with accompanying solvents may align themselves at or near the double layer are shown in Figure 11. Frumkin suggested the possibility of Coulombic type cationic bridges within the double layer [18]. But there was no convincing evidence as to the nature of the alignment. Similarly Devanathan and Fernando had suggested the formation of "anionic bridges" between tetra alkylammonium ions and iodide ions in order to explain the electrocapillary data [19]. However these authors have not discussed the specific alignment of these ion pairs at or near the electrode.

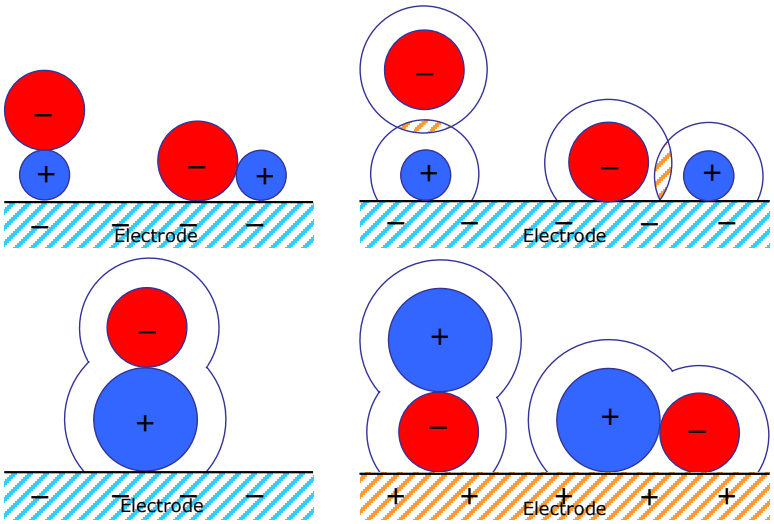

Figure 11. Anionic and cationic bridges at the electrode.

The relationship between the three dimensional solution concentrations in the bulk and the two-dimensional ionic concentrations at an electrode interface is given by the equation [20]:

$$C_i = \check{T}_i^{3/2} N^{1/2} 1000 \text{ mol dm}^{-3}$$
$$= (q_i/F)^{3/2} N^{1/2} 1000 \text{ mol dm}^{-3}$$

where $\check{T}_i$ = 2-dimensional surface concentration in mol cm^{-2} of an ion of type i in the interphase; C_i = the equivalent 3-dimensional concentration; q_i is the adsorbed ion charge in the inner layer, C m^{-2}; N = Avogadro's number. From this, it is seen that for $\pm q_i = 0.05$, $\check{T}_i = 5.19$ and $C_i = 0.50$. It is seen that the

2-dimensional surface concentration is about 10 times higher than the bulk 3-dimensional concentration. One has to keep this in mind when one considers the interionic effects as well as the co-sphere overlap effects in dilute bulk electrolyte solutions.

The double layer models of Gouy, Stern, Frumkin, Grahame, Chapman, and their extensions have been investigated and reviewed in great detail in the past [21-25]. In the simplest case, the charge on the metal may be separated from the charge on the solution by a monolayer of water. The amount of free water, of hydration co-spheres and of the overlaps of the hydration co-spheres depends on the nature of ions as well as of ion concentrations. Information on the nature of the double layer has been obtained mostly from double layer capacitance measurements and electrocapillary measurements of simple electrolytes.

Friedman and his colleagues have used the ion hydration co-sphere overlap model, as shown in Figure 12, and statistical mechanical models, to compute the activity coefficient data of 1:1 electrolytes and Setchenow coefficients [26-28].

Conway has used this concept of co-sphere overlap, as shown in Figure 13, to explain ion-hydration co-sphere interactions in the double layer in the presence of tetrapropyl ammonium ions [20]. He suggested three kinds of ion hydration co-sphere overlap regions in the double layer:
"a) Lateral co-sphere overlap between hydration shells of specifically adsorbed ions; b) Ion hydration co-sphere overlap with the co-plane of oriented solvent due to electrode surface charge, and c) Possible co-sphere overlap with ions in the diffuse layer."

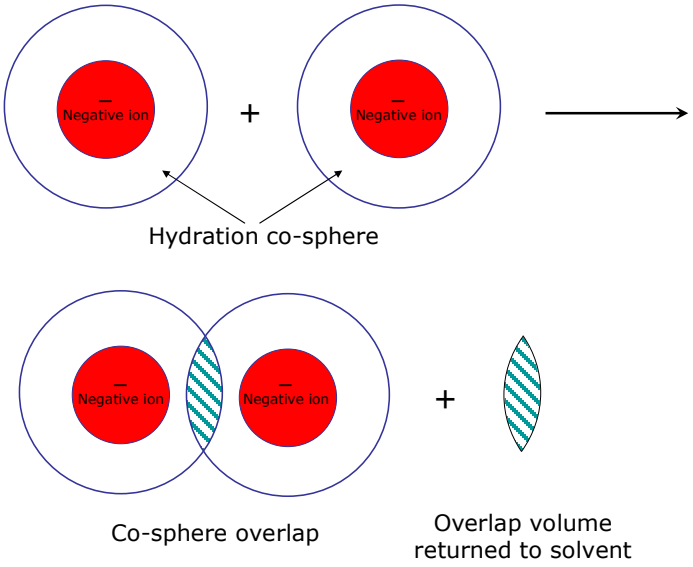

Figure 12. Gurney ion hydration co-sphere overlap.

To explain our admittance data, especially those shown in Figures 8 and 9 we propose a new model, "potential induced and water structure-enforced ion-pair formation". During admittance measurements, when the potential changes from negative to less negative, less negative to zero, and finally to positive, the orientation of the positively charged sodium towards mercury has to gradually

change and finally negatively charged chloride ions have to orient towards mercury. During this process the accompanying water in the hydration layer as well as in the monolayer, if any, near mercury, has also to change their orientation from hydrogen to oxygen.

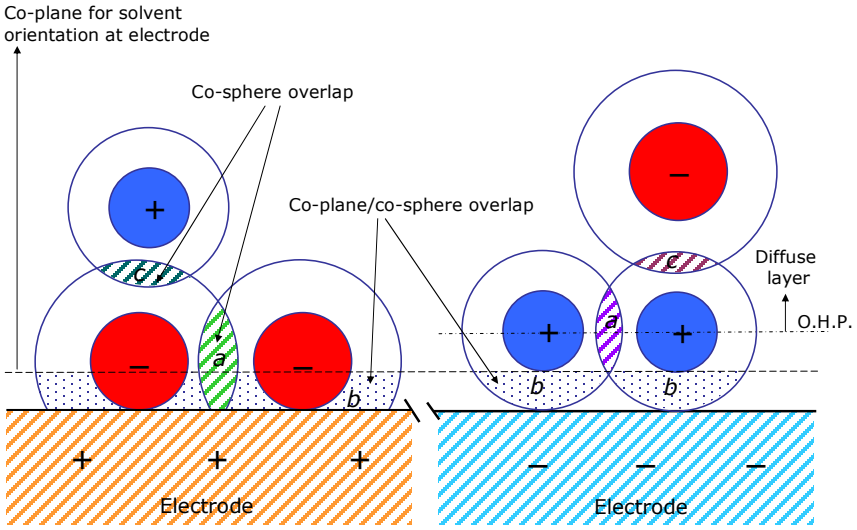

Figure 13. Gurney ion hydration co-sphere overlap regions in the double layer [adapted from ref. 20].

To minimize the disturbance of the water structure, it is preferable to have the sodium ion and the halide ion forming an ion-pair either of the localized hydrolysis type (depending on the anion) or the water structure-enforced type. This water structure-enforced type ion-pair is slightly different from the one postulated in the literature where only two large ions are forced to form this type of ion pair. The potential induced and the water structure-enforced ion-pair formation does not need to have this criterion. This type of ion formation would explain the observed decrease in admittance at potentials in the cathodic range. Whereas the ion-pair formation, no matter which type, is observed in bulk electrolytes only at high concentrations, our admittance data indicate that they are formed even in very dilute solutions, as shown in Figure 8(right side). These ion-pairs are formed at higher cathodic potentials with decreasing concentration.

These ion-pairs, being symmetrical, have no net charge and will not make any contribution to the electrical conductivity. There are different water orientations around this ion pair because of a possible dipole moment for the ion-pair. The fluctuations in these orientations may partly account for the frequency dependent admittance.

The admittance data in Figure 9 suggest that the ion-pair formation is in the order NaI > NaBr > NaCl > NaF. This order is consistent with the order expected for water structure-enforced ion-pair formation. However, this order was the reverse of the order of the osmotic and activity coefficient behavior observed for the bulk electrolyte. We wish to point out that this behavior is not related to the interaction of mercury with halides because the current observations are at highly cathodic regions and nowhere near the passivation region.

Finally we would like to briefly mention the consequences of the proposed model on the models used to explain differential capacitance and surface excess entropy data.

In the absence of specific adsorption, the measured capacitance of the double layer C [29-30] is commonly attributed to two capacitors connected in series, the inner layer C_i and the diffuse layer C_d:

$$1/C = 1/C_i + 1/C_d = [r/(\varepsilon_i\varepsilon_o) + (a\text{-}r)/(\varepsilon_{IHP\text{-}OHP}\varepsilon_o)] + (1/\kappa)/(\varepsilon\varepsilon_o)$$

where ε_i is the electric permittivity of solvent at the surface, ε_o is the electric permittivity of a vacuum, r is the inner layer thickness, a is the outer Helmholtz layer thickness, $\varepsilon_{IHP\text{-}OHP}$ is the permittivity of the solvent between the inner and outer Helmholtz planes, ε is the permittivity of the solvent in the bulk, and $1/\kappa$ is the Debye length [31-32]. A two-orientational state model in which the water dipole can have two components in the direction normal to the metal surface and a modified form of this with a four state model where the water molecules are considered as small clusters (of 3-4) and free molecules have been proposed to explain these data. The entropy of formation of the mercury-NaF system has been explained using the two state model [33-35]. The entropy contributions are attributed to the monolayer of water molecules in the inner region between the mercury surface and the distance of closest approach of nonadsorbed ions. The maximum in entropy occurs at a surface charge of – 4 μCcm^{-2}. A "hump" is observed in the plot of the electrical double layer capacity between mercury and aqueous solutions versus polarization potential or surface charge density. The minimum in the differential capacitance occurs around a surface charge density of –12 μCcm^{-2}. Controversies exist between different models because the "hump" in differential capacity does not coincide with the maximum in entropy.

There are conflicting experimental and theoretical results on the effect of electric field on the dissociation of solutes in the electrical double layer [36-43]. Theories of Gouy-Chapman [21-22], Onsager [41] and dissociation field effect [37-38, 42-43] have been used to explain the dissociation (the correct term should be ionization and not dissociation) rate constants of weak acids [38, 40-43] in the electrical double layer. At the potential of zero charge (pzc), the electric field intensity being the lowest, allows water molecules to adsorb as clusters. When the electrode is polarized on either side of pzc, the water clusters can break up due to their changing interaction with the electrode. The orientation of water molecules also will be different on either side of pzc. All of these will contribute to the observed admittance.

Another factor that will influence the admittance at low frequencies is the electric permittivity of water in the inner part of the double layer (about 6 when measured at 10^8 Hz compared to 78 in the bulk due to lack of the dipole correlation effects). These values are dependent on the frequency of measurements as well as the surface charge and it is known that this reduction is much less at low frequencies [32]. The varying nature of admittance at different concentrations and different frequencies may partly be due to the well known [44] but complicated fashion in which the dielectric constant varies with frequency.

Another interaction that one has to consider is the magnitude of the dipole-dipole interaction in water (~0.25 $x10^{-19}$ J) and the charge-dipole interaction (~1 $x10^{-19}$ J). These differences contribute to a

change in the solvent structure and its dielectric properties at the interface. The formation of ion-pairs changes the magnitude of the charge-dipole interaction.

We are not aware of any experimental or theoretical work dealing with the influence of electric field on ion pair formation of simple and strong monovalent electrolytes in water. Our admittance results at different frequencies and concentrations suggest the need to reevaluate the different models suggested for explaining the electrical double layer.

4. CONCLUSIONS

Our admittance data at different concentrations of sodium chloride suggest the formation of potential induced and water structure-enforced ion-pair formation at or near the double layer. This kind of ion-pair formation was observed even in very dilute solutions, unlike the classical Bjerrum-type Coulombic ion pairs observed in concentrated solutions of bulk electrolytes. The potential induced and water structure-enforced ion pair formation was in the order NaI > NaBr > NaCl > NaF, and was the reverse of the order of the osmotic and activity coefficient behavior observed for the bulk electrolyte. Finally, the admittance has provided much complimentary information to the differential capacitance and electrocapillary data.

ACKNOWLEDGMENTS

B. Chu acknowledges financial support of this work provided by the Basic Energy Sciences, Department of Energy (DEFG0286ER45237). We also thank Dr. Rafael Muńoz-Espi for help with some figures.

References

1. C.V. Krishnan and M. Garnett, *Int. J. Electrochem. Sci.,* 1 (2006) 215
2. C.V. Krishnan and M. Garnett, *Int. J. Electrochem. Sci.,* 1 (2006) 283
3. C.V. Krishnan and M. Garnett, *Electrochimica Acta,* 51 (2006) 1541
4. M.A.V. Devanathan and P. Peries, *Trans. Faraday Soc.,* 50 (1954) 1236
5. D.C. Grahame and R. Parsons, *J. Am. Chem. Soc.,* 83 (1961) 1291
6. D.C. Grahame, *J. Am. Chem. Soc.,* 80 (1958) 4201
7. R. Payne, *Trans. Faraday Soc.,* 64 (1968) 1638
8. C.V. Krishnan, M. Garnett, B. Hsiao and B. Chu, *Int. J. Electrochem. Sci.,* 2 (2007) 29
9. C.V. Krishnan, M. Garnett and B. Chu, *Int. J. Electrochem. Sci.,* 2 (2007) 444
10. J.E. Bauerle, *J. Phys. Chem. Solids,* 30 (1969) 2657
11. R.A. Robinson and R.H. Stokes, *Electrolyte Solutions,* Second edition, Academic Press, New York (1959)
12. R.M. Fuoss, *J. Am. Chem. Soc.,* 80 (1958) 5059
13. R.A. Robinson and H.S. Harned, *Chem. Rev.,* 28 (1941) 419
14. R.M. Diamond, *J. Am. Chem. Soc.,* 80 (1958) 4808
15. R. M. Diamond, *J. Phys. Chem.,* 67 (1963) 2513
16. V.T. Athavale, C.V. Krishnan and Ch. Venkateswarlu, *Indian J. Chem.,* 5 (1967) 496
17. C.V. Krishnan and P.S. Ramanathan, *Indian J. Chem.,* 5 (1967) 551
18. A.N. Frumkin, *Trans. Faraday Soc.,* 55 (1959) 156

19. M.A.V. Devanathan and M.J. Fernando, *Trans. Faraday Soc.,* 58 (1962) 368
20. B.E. Conway, *J. Electroanal. Chem.,* 123 (1981) 81
21. D.C. Grahame, *Chem. Rev.,* 41 (1947) 441
22. D.C. Grahame, *Ann. Rev. Phys. Chem.,* 6 (1955) 337
23. M.A.V. Devanathan and B.V.K.S.R.A. Tilak, *Chem. Rev.,* 65 (1965) 635
24. S. Trasatti and E. Lust, *Modern Aspects of Electrochemistry,* Edited by R.E. White, J.O'M. Bockris and B.E. Conway, Kluwer Academic/Plenum Publishers, Vol. 33, NewYork (1999)
25. R. Parsons, *Chem. Rev.,* 90 (1990) 813
26. P.S. Ramanathan, C.V. Krishnan and H.L. Friedman, *J. Solution Chem.,* 1 (1972) 237
27. P.S. Ramanathan and H. L. Friedman, *J. Chem. Phys.* 54 (1971) 1086
28. C.V.Krishnan and H.L. Friedman, *J. Solution Chemistry,* 3 (1974) 727
29. D.C. Grahame, *J. Chem. Phys.,* 23 (1955) 1725
30. R. M. Reeves, *Modern Aspects of Electrochemistry,* Edited by B.E. Conway and J.O'M. Bockris, Plenum Press, Vol. 9, New York (1974)
31. P.A. Christensen and A. Hamnett, *Techniques and Mechanisms in Electrochemistry, Chapman* & Hall, London (1994)
32. J. Sobkowski and M.J. Herbich, *Modern Aspects of Electrochemistry,* Edited by J.O'M. Bockris, R. E. White and B.E. Conway, Plenum Press, Vol. 31, New York (1997)
33. J.A. Harrison, J.E.B. Randles and D.J. Schiffrin, *J. Electroanal.Chem.,* 48 (1973) 359
34. G.J. Hills and S. Hsieh, *J. Electroanal. Chem.,* 58 (1975) 289
35. I.L. Cooper and J. A. Harrison, *J. Electroanal. Chem.,* 66 (1975) 85
36. H.W. Nurnberg and G. Wolff, *J. Electroanal. Chem.,* 21 (1969) 99
37. K. Takahashi and R. Tamamushi, *Electrochim. Acta,* 16 (1971) 875
38. A. Sanfeld and A. Steinchen-Sanfeld, *Trans. Faraday Soc.,* 62 (1966) 1907
39. H.D. Hurwitz, A. Sanfeld and A. Steinchen-Sanfeld, *Electrochim. Acta,* 9 (1964) 929
40. H.W. Nurnberg, *Discuss. Faraday Soc.,* 39 (1965) 136
41. L. Onsager, *J. Chem. Phys.,* 2 (1934) 599
42. L. Bass, *Trans. Faraday Soc.,* 62 (1966) 1900
43. G.G. Susbielles and P. Delahay, *J. Phys. Chem.,* 72 (1968) 841
44. A. Shadowitz, *The Electromagnetic Field,* Dover Publications, New York (1975)